1521-0103/369/1/67–77$35.00
THE JOURNAL OF PHARMACOLOGY AND EXPERIMENTAL THERAPEUTICS

https://doi.org/10.1124/jpet.118.255216
J Pharmacol Exp Ther 369:67–77, April 2019

RLA8—A New and Highly Effective Quadruple PPAR-$\alpha/\gamma/\delta$ and GPR40 Agonist to Reverse Nonalcoholic Steatohepatitis and Fibrosis[S]

Meng Hua Li, Wei Chen, Li Li Wang, Jia Lin Sun, Lei Zhou, Yu Cong Shi, Chu Han Wang, Bo Hua Zhong, Wei Guo Shi, and Zhong Wu Guo

National Glycoengineering Research Center and Shandong Provincial Key Laboratory of Carbohydrate Chemistry and Glycobiology, Shandong University, Jinan, People's Republic of China (M.H.L., Z.W.G.); State Key Laboratory of Toxicology and Medical Countermeasures, Beijing Institute of Pharmacology and Toxicology, Beijing, People's Republic of China (M.H.L., W.C., L.L.W., J.L.S., L.Z., B.H.Z., W.G.S.); Capital Medical University School of Basic Medical Sciences, Fengtai District, Beijing, People's Republic of China (Y.C.S., C.H.W.); and Teizhou Huayuan Med Tech Company LTD, Taizhou, People's Republic of China (B.H.Z.)

Received November 19, 2018; accepted February 1, 2019

ABSTRACT

Nonalcoholic fatty liver disease (NAFLD) is a very common chronic hepatic disease, with nonalcoholic steatohepatitis (NASH) as a major and severe subcategory that can lead to cirrhosis and hepatocellular carcinoma, and thereby to a high mortality rate. Currently, there has been no approved drug to treat NAFLD or NASH. The current study has presented RLA8, a novel and balanced quadruple agonist for hepatic lipid metabolism and inflammation-related peroxisome proliferator-activated receptors (PPARs)-$\alpha/\gamma/\delta$ and G protein–coupled receptor 40 (GPR40), as a NASH drug candidate. The efficacy of RLA8 to treat NASH was evaluated in vivo using two mouse models induced by methionine/choline-deficient diet or by high-fat diet, respectively. RLA8 was shown to improve serum alanine aminotransferase and high-density lipoprotein cholesterol levels, reduce hepatic free fatty acid and triglyceride levels, and alleviate insulin resistance. Cytokine and lipoperoxide analysis revealed that RLA8 could reduce oxidative stress and inflammation. Histochemical and morphologic examination of mouse livers showed that RLA8 could improve pathologic changes such as steatosis, ballooning, collagen fiber, and inflammation. Polymerase chain reaction and Western blot analyses proved that RLA8 could result in PPARs and GPR40 activation, accompanied by upregulation of the 5′AMP-activated protein kinase-acetyl-CoA carboxylase pathway and inhibition of the expression of lipogenic genes and proteins, which provided more insights into its action mechanisms. In summary, RLA8 has significantly better efficacy to improve NASH-induced liver damage such as steatosis, inflammation, and fibrosis, and, consequently, it represents a new and highly promising NASH drug candidate that is worthy of further investigation and development.

Introduction

Nonalcoholic fatty liver disease (NAFLD) is a common chronic hepatic disease associated with fat accumulation in the liver, which leads to hepatocyte damage and inflammation with or without fibrosis. Nonalcoholic steatohepatitis (NASH) is a major and severe subcategory of NAFLD characterized by the presence of hepatic vesicular steatosis, hepatocyte balloon degeneration, inflammation, and fibrosis (Chalasani et al., 2012). It is estimated that about one-quarter of the world population is affected by NAFLD and 3%–5% is suffering from NASH (Vernon et al., 2011; Williams et al., 2011). Furthermore, cirrhosis and hepatocellular carcinoma eventually develop in approximately 15%–20% of NASH patients, resulting in a high mortality rate (Adams et al., 2005; Ekstedt et al., 2006). Therefore, NAFLD, especially NASH, represents a major and ever-growing social, economic, and health problem worldwide.

Unfortunately, there have been no drugs approved for the treatment of NASH yet, although several drug candidates are

This work was supported by a Science and Technology Development Project of Shandong Province [No. 2016GGH4502] and partially supported by the National Natural Science Foundation of China [No. 81773790] and the National Science and Technology Major Project of the Ministry of Science and Technology of China [Grant no. 2012ZX09301-003]. M.H.L. and Z.W.G. have received funding from Shandong Province.
https://doi.org/10.1124/jpet.118.255216.
[S] This article has supplemental material available at jpet.aspetjournals.org.

ABBREVIATIONS: ACC, acetyl-CoA carboxylase; ALT, alanine aminotransferase; AMPK, 5′AMP-activated protein kinase; FAS, fatty acid synthase; FFA, free fatty acid; FXR, farnesoid X receptor; GAPDH, glyceraldehyde-3-phosphate dehydrogenase; GPR40, G protein-coupled receptor 40; HDL-C, high-density lipoprotein cholesterol; HFD, high-fat diet; HOMA-IR, homeostasis model of assessment for insulin resistance; IL, interleukin; MC, model control; MCD, methionine and choline–deficient diet; NAFLD, nonalcoholic fatty liver disease; NAS, nonalcoholic fatty liver disease activity score; NASH, nonalcoholic steatohepatitis; NC, normal control; OCA, obeticholic acid; p, phosphorylated; PCR, polymerase chain reaction; PPAR, peroxisome proliferator-activated receptor; RSV, resveratrol; SCD1, stearyl-CoA desaturase 1; SREBP1, sterol regulatory element-binding protein 1; TC, total cholesterol; TG, triglyceride; TGFβ1, transforming growth factor β1; TIMP1, tissue inhibitor of metalloproteinases 1; TNF-α, tumor necrosis factor α; VCAM1, vascular cell adhesion molecule 1.

being investigated in clinical trials. Among them, obeticholic acid [OCA (INT-747; $C_{26}H_{44}O_4$)] and elafibranor (GFT-505; $C_{22}H_{24}O_4S$) are the most representative and hopeful candidates currently in an advanced stage of (phase III) clinical development (Neuschwander-Tetri et al., 2015; Ratziu et al., 2016). OCA is a bile acid derivative and a transcriptional activator of the nuclear farnesoid X receptor (FXR) (Pellicciari et al., 2002), which has already been approved for treating primary biliary cholangitis (Markham and Keam, 2016). Preliminary results from National Institutes of Health–sponsored FLINT (Farnesoid X Nuclear Receptor Ligand Obeticholic Acid for Non-Cirrhotic, Non-Alcoholic Steatohepatitis) clinical trials of OCA as a NASH drug revealed that it had significant beneficial effects on NASH-induced liver damage, such as ameliorating steatosis, inflammation, and fibrosis (Neuschwander-Tetri et al., 2015). However, OCA treatment was associated with an increase in the frequency and severity of pruritus, a major adverse effect of OCA. Moreover, OCA-treated patients also displayed an increase in total cholesterol (TC) and low-density lipoproteins and a decrease in high-density lipoproteins (HDLs) (Ratziu et al., 2016).

Elafibranor is a selective dual agonist for peroxisome proliferator–activated receptors (PPARs) α and δ (Cariou et al., 2013), which belong to another family of ligand-activated nuclear receptors that play a key role in the regulation of metabolism and inflammation and whose stimulation was shown to ameliorate NAFLD (Hansen et al., 2017). Elafibranor has been demonstrated to reduce hepatic fat accumulation, inflammation, and fibrosis in preclinical and clinical studies, making it a promising NAFLD and NASH drug candidate (Ratziu et al., 2016). Its main side effect was to cause a mild increase in serum creatinine in most subjects (Gawrieh and Chalasani, 2018). Besides elafibranor, several other PPAR subtype–selective agonists, like fibrates such as PPAR-α ligands, thiazolidinediones such as PPAR-γ ligands, and GW501516 ($C_{21}H_{18}F_3NO_3S_2$) as a PPAR-δ ligand, have also been explored and were demonstrated to reduce fibrotic steatohepatitis in the methionine and choline–deficient (MCD) diet-induced mouse NASH model (Hansen et al., 2017).

Our group has recently explored a new NASH drug design, aiming at activating multiple related receptors with one agonist (Li et al., 2012). As a result, we discovered ZBH as a potent and balanced triple agonist for PPAR-$\alpha/\gamma/\delta$ (Chen et al., 2014). Recently, we also become interested in G protein–coupled receptor 40 [GPR40 (also known as FFAR1)] expressed in both pancreatic β-cells and hepatocytes (Suh et al., 2008; Ou et al., 2013), because a recent study has revealed that GPR40 activation could improve high-fat diet (HFD)–induced hepatic steatosis in mice (Ou et al., 2014). It was further demonstrated that medium and long chain fatty acids could activate GPR40 (Briscoe et al., 2003). Accordingly, we designed and synthesized a series of new agonists containing the key structural and pharmacophore motifs of PPAR-$\alpha/\gamma/\delta$ agonists, such as elafibranor, fibrates, and resveratrol (RSV), which is also an anti-inflammatory and antiatherogenic agent (Cavallaro et al., 2003; Li and Kazgan, 2011; Nakata et al., 2012), as well as the structural motif of GPR40 agonists, that is, a long chain fatty acid. Our preliminary screening showed that RLA8 (Fig. 1) was a promising quadruple agonist. We present herein a detailed investigation of its PPARs and GPR40 agonist activities, its action mechanism, and its influences on NASH and fibrosis by in vitro transactivation assays and using mouse NASH models generated from different pathologic mechanisms.

Materials and Methods

In Vitro Transactivation Assays. RSV, OCA, ZBH, and RLA8 were synthesized and provided by the New Drug Design Center of Beijing Institute of Pharmacology and Toxicology. Their purities and structures were determined and confirmed by high-performance liquid chromatography, mass spectrometry, and NMR spectrometry. Purity of the compounds used in all experiments was more than 98%. All plasmids used in the transactivation assays were provided by the Lili Wang Laboratory of Beijing Institute of Pharmacology and Toxicology. Transactivation assays of RLA8 and ZBH toward PPARs, GPR40, GPBAR1 (G protein bile acid receptor 1), and FXR were performed according to previously described protocols (Xu and Xie, 2009; Chen et al., 2014; Gao et al., 2018). The EC_{50} value was obtained by analysis of the data using GraphPad Prism software (GraphPad Software, San Diego, CA).

Animals, Diets, and Treatment Schemes. Adult male C57BL/6J mice, weighing 24 ± 2 g, purchased from the Vital River Laboratory Animal Technology Co. Ltd. (Beijing, People's Republic of China) were used in this work. Animal breeding and care were provided by the Animal Care Facility of Beijing Institute of Pharmacology and Toxicology. All of the animal experiments were carried out according to an animal protocol approved by the Animal Experimental Ethics Committee of the Beijing Institute of Pharmacology and Toxicology in strict accordance with the current Animal Protection Law of China. The mice were allowed to have free access to water and food, and were kept at 21 ± 2°C with a relative humidity of 60% ± 10% and illumination for 12 h/day (8:00 AM to 8:00 PM). MCD diet (catalog number TP3005) was purchased from Trophic Animal Feed High-Tech Co., Ltd., China (Nantong, People's Republic of China), and HFD diet (60% kcal from fat; catalog number D12492) was purchased from Research Diets (New Brunswick, NJ).

After mice arrived at the animal facility, they were acclimated for 1 week. Thereafter, they were fed with an MCD diet for 6 weeks or an HFD diet for 12 weeks to induce NASH. At the end of the 6th or 12th week, the mice were randomly divided into four groups that received treatments with RSV (100 mg/kg) (Heebøll et al., 2015), OCA (10 mg/kg) (Rodrigues et al., 2017), RLA8 (100 mg/kg), and saturated $NaHCO_3$ solution (0.1 ml/10 g), respectively. All drugs were administered through gavage once a day for 3 weeks for the MCD model and 4 weeks for the HFD model. Mice having standard rodent diets were used as the normal control (NC). Individual body weight and cage food consumption were measured once a week. At the end of the experiments, the mice were anesthetized with isoflurane and then euthanized with carbon dioxide for the collection of blood and liver samples.

Biochemical Assays. Mouse serum biochemical indices, including alanine aminotransferase (ALT), glucose, HDL cholesterol (HDL-C), liver triglyceride (TG), TC, and free fatty acid (FFA), were examined using an automatic biochemical analyzer (Modular-PPI, Roche, Switzerland). Insulin, lipoperoxides, interleukin (IL)-6, IL-10, and tumor necrosis factor α (TNF-α) were analyzed with ELISA kits, according to the manufacturer instructions. The homeostasis model of assessment for insulin resistance (HOMA-IR) was calculated based on the values of fasting blood glucose (FBG) and fasting blood insulin (FINS) according to the following equation: HOMA-IR = FBG × FINS/22.5 (Matthews et al., 1985).

Histochemical and Morphologic Studies. Liver samples were fixed in 4% paraformaldehyde, and the paraffin-embedded sections (2–3 μm) were stained with H&E, Oil Red O, or Masson's Trichrome. The sections were then scored blindly by two experienced pathologists according to the NAFLD activity score standards listed in Table 1 (Kleiner et al., 2005). Tissues with a total score of NAFLD activities greater than 5 were diagnosed as NASH, and those with a score of less than 3 were diagnosed as "none NASH."

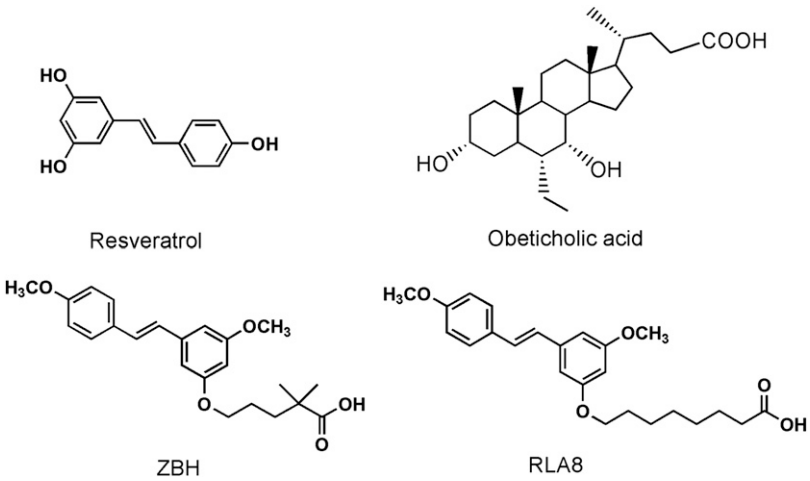

Fig. 1. The chemical structure of RSV, OCA, ZBH, and RLA8.

Analysis of Target Genes by Quantitative Real-Time Polymerase Chain Reaction. Total RNA of the liver samples was extracted with the reverse transcription kit (Promega, Madison, WI) to obtain the first-strand cDNA. Then, quantitative real-time polymerase chain reaction (PCR) was performed under the following conditions: 2 minutes at 95°C, followed by 40 cycles for 15 seconds at 95°C, 15 seconds at 60°C, and 30 seconds at 72°C. The primers used these studies are shown in Supplemental Table 1, and glyceraldehyde-3-phosphate dehydrogenase (GAPDH; National Center for Biotechnology Information Reference Sequence NM_031144) was included as an internal control. Each sample was performed in triplicate. Standard curves were generated from five repeated 10-fold serial dilutions of cDNA, and the copy numbers of target genes in every milliliter of the sample were calculated according to the standard curve (Li et al., 2014).

Analysis of Target Proteins by Western Blotting. Western blot was performed according to the protocols of Towbin et al. (1979). Proteins derived from cells or tissues were separated by SDS-PAGE and then transferred to an Immobilon-P membrane (Millipore, Burlington, MA). Thereafter, the membrane was blocked with 5% nonfat milk in 0.1% Tween 20 at room temperature for 1 hour and then incubated with the respective primary antibody against 5′AMP-activated protein kinase (AMPK), phosphorylated (p) AMPK (Thr172), acetyl-CoA carboxylase (ACC), p-ACC (Ser79), sterol regulatory element-binding protein 1 (SREBP1), fatty acid synthase (FAS), stearyl-CoA desaturase 1 (SCD1), tissue inhibitor of metalloproteinases 1 (TIMP1), vascular cell adhesion molecule 1 (VCAM1), or transforming growth factor β1 (TGFβ1) (Cell Signaling Technology Inc., Shanghai, People's Republic of China) at 4°C overnight. The membrane was washed with Tris-buffered saline containing Tween 20 for 30 minutes and then incubated with the secondary antibody horseradish peroxidase–conjugated goat anti-rabbit IgG (Jackson ImmunoReseach Laboratories Inc., Beijing, People's Republic of China) at room temperature. Proteins were visualized using enhanced chemiluminescence reagents (Millipore). Protein content analysis was carried out using ImageQuant TMTL software (GE Healthcare Life Sciences, Pittsburgh, PA).

Statistical Analysis of Experimental Results. All data were expressed as the mean ± S.D. One-way analysis of variance followed by the least significant difference test was used to compare experimental values between groups, with $P < 0.05$ being considered as statistically significant.

Results

Evaluation of RLA8 as a PPAR and GPR40 Agonist. RLA8 is a completely novel class of anti-NASH drug. It was designed to carry the key structural and pharmacophore motifs of elafibranor, fibrates, and RSV as a triple agonist for PPAR-α/γ/δ and a long chain fatty acid moiety as a GPR40 agonist. To confirm its quadruple agonist property, RLA8 was subjected to in vitro transactivation assays using all three subtypes of PPARs and GPR40 by previously described protocols (Xu and Xie, 2009; Chen et al., 2014). Its EC_{50} values as a PPAR-α, PPAR-δ, PPAR-γ, and GPR40 agonist were 7.04, 18.89, 18.65, and 1.27 μM, respectively (Table 2). The results were compared with that of ZBH, a pan-PPAR agonist that was demonstrated in vitro to possess relatively balanced agonist activities for PPAR-α/γ/δ but weak activity for GRP40. ZBH was also shown in vivo to significantly decrease TGs and to have more potent hypolipidemic activity than fenofibric acid (Chen et al., 2014).

Clearly, RLA8 showed relatively strong and comparable agonist activities for all three subtypes of PPARs and GPR40. For example, its EC_{50} value for PPAR-α was only 2.6-fold and 4.1-fold better than that for PPAR-δ and PPAR-γ, suggesting more balanced PPAR pan-agonist activities than ZBH, which had some PPAR-α preference (11.0-fold and 14.5-fold better than for PPAR-δ and PPAR-γ) (Chen et al., 2014). More importantly, compared with ZBH, RLA8 displayed 192-fold

TABLE 1
Histologic scoring system for NASH

Score	Steatosis	Inflammation	Ballooning Degeneration
	%		
0	<5	No foci	None
1	5–33	<2 foci per 200 × field	Few
2	33–66	2–4 foci per 200 × field	Many
3	>66	>4 foci per 200 × field	

TABLE 2
The agonist activities of RLA8 and ZBH for PPARs and GPR40
Values are the mean ± S.D. obtained from three independent experiments.

Compound	EC_{50}			
	PPARα	PPARδ	PPARγ	GPR40
	μM			
RLA8	7.04 ± 1.60	18.89 ± 1.53	28.65 ± 2.04	1.27 ± 0.09
ZBH	1.75 ± 0.12	19.19 ± 0.77	25.35 ± 1.97	244.4 ± 21.06

better agonist activity toward GPR40 (EC_{50} values, 1.27 vs. 244.4 μM), suggesting that RLA8 is indeed a quadruple agonist.

The Influence of RLA8 Treatment on the Body Weight and Food Intake of NASH Mice. There are two common animal models established to study NASH. One is the diet-induced obesity model or HFD-induced model, which mimics the natural process of NASH and represents NASH with histopathologically mild to moderate liver fibrosis, accompanied with obesity and insulin resistance (Marin et al., 2016). The other is an MCD diet–induced model, which is the more reproducible NASH model. With the diet model devoid of an essential amino acid, methionine, and choline in the diet promotes the occurrence of severe liver fibrosis and significant weight loss, making it more appropriate for the study of histologically advanced NASH (Weltman et al., 1996, 1998; Machado et al., 2015; Lau et al., 2017). We used both models to investigate the efficacy of RLA8 for the treatment of NASH and related diseases.

First, we evaluated the influence of RLA8 on the body weight and food intake of MCD and HFD mice. As described in the experimental section, after C57BL/6J mice were fed with an MCD diet for 6 weeks or with an HFD diet for 12 weeks, they started to receive treatments with RSV (100 mg/kg) (Heebøll et al., 2015), OCA (10 mg/kg) (Rodrigues et al., 2017), and RLA8 (100 mg/kg), respectively, or with saturated $NaHCO_3$ (0.1 ml/10 g) as the model control (MC). Mice fed with standard rodent diets were used as the NC. The dose regimen for RLA8 was established in a pilot study using a 4-week MCD-fed mouse model, where significant reduction in hepatic lipids was observed. All compounds were administered through gavage once a day for 3 weeks in the MCD model, and for 4 weeks in the HFD model. Individual body weight and cage food consumption were measured once a week, and the results are depicted in Fig. 2 and Supplemental Table 2. Clearly, compared with those of NC mice, the body weights of MCD mice in the MC group decreased significantly, which lasted until the end of the experiments, indicating the occurrence and development of NASH symptoms (Fig. 2A). Delightfully, after RLA8 treatment, the body weight loss was halted, and a statistically significant difference in the body weight between RLA8 and MC groups was observed 1 week after RLA8 administration ($P < 0.05$) (Fig. 2A). RSV and OCA treatments showed a similar impact on mouse body weight, but their difference from the MC group was not statistically significant. These results indicated that RLA had better or at least similar activities to inhibit body weight loss in MCD mice, compared with the positive controls RSV and OCA.

In contrast to the MCD model, HFD caused a significant increase in the body weights of the MC mice compared with NC mice ($P < 0.01$) (Fig. 2C). RLA8 and OCA treatments had similar effects to invert excessive body weight gain. Their difference from the MC group was statistically very significant ($P < 0.01$) (Fig. 2C). RSV treatment could also stop mice from gaining more body weight, and its difference from the MC group was statistically significant ($P < 0.05$) (Fig. 2C). However, the efficacy of RSV was not as high as that of RLA8 and OCA. In addition, all three compounds did not show a significant impact on food intake by mice of both models (Fig. 2B; Fig. 3D).

The Influence of RLA8 Treatment on the Morphology of MCD and HFD-Induced NASH. Once the livers of the

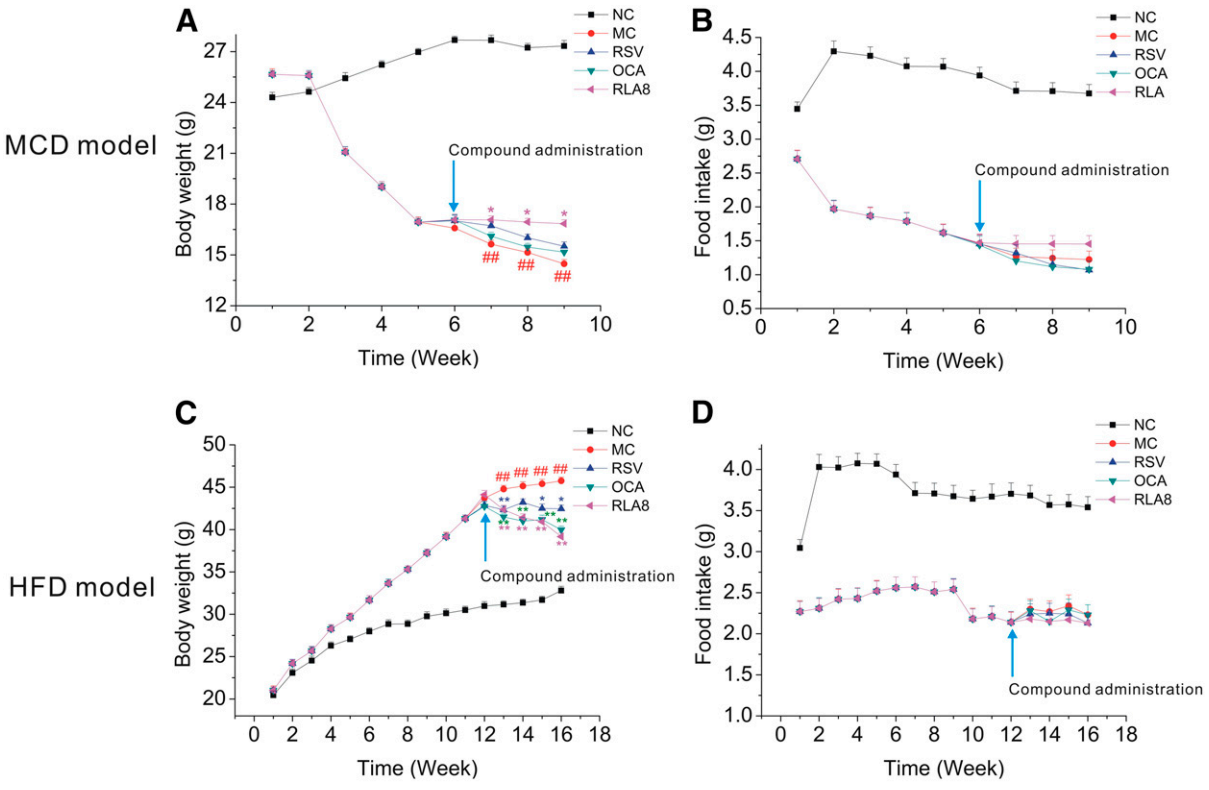

Fig. 2. The influences of RLA8, RSV, and OCA on the body weight change (A and C, averaged) and food intake (B and D, averaged) in MCD- and HFD-induced NASH mice. Values are the mean ± S.D. (n = 10 mice/group). ##$P < 0.01$ compared with NC; *$P < 0.05$; **$P < 0.01$ compared with MC.

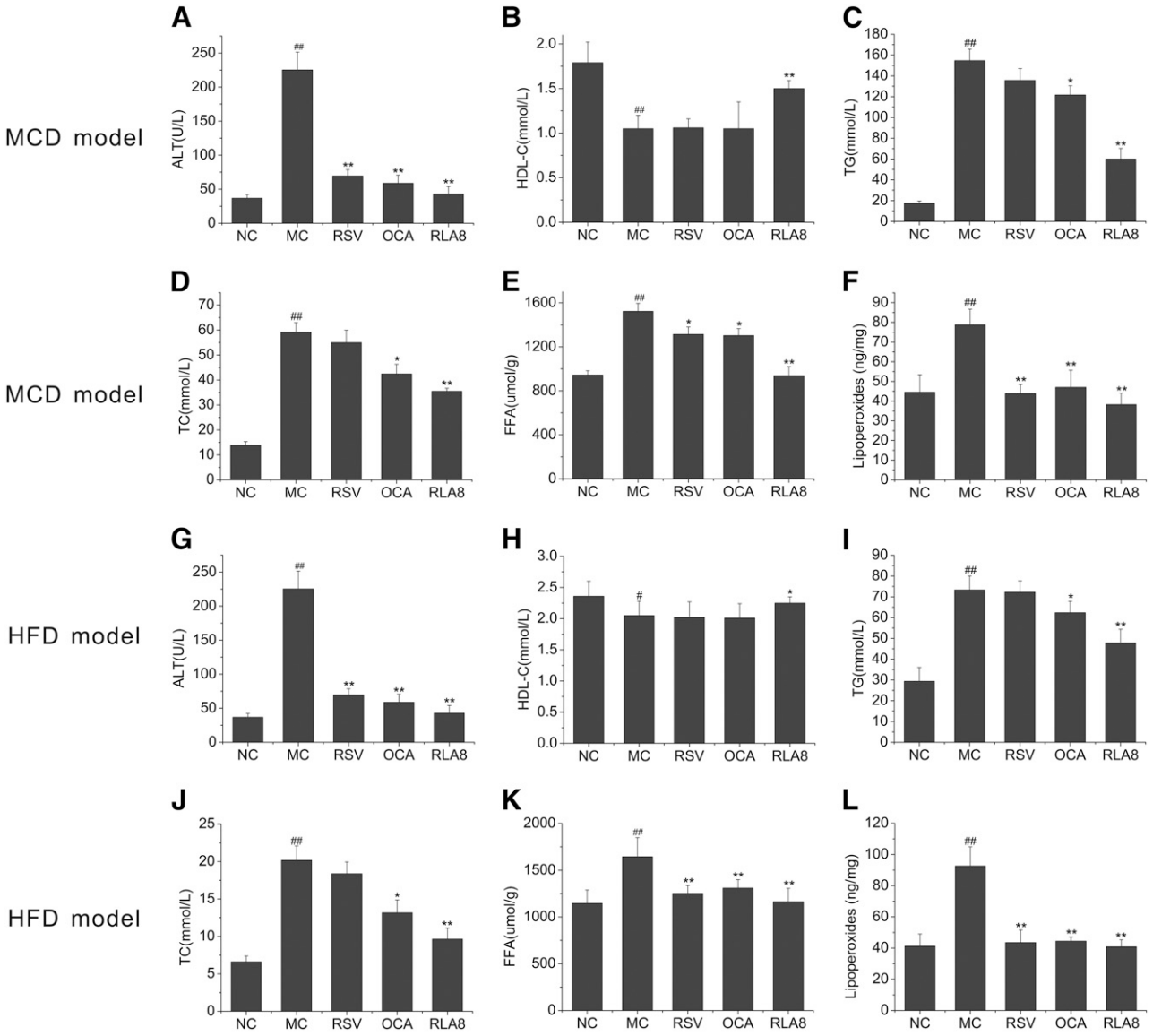

Fig. 3. The influence of RLA8, RSV, and OCA treatments on serum levels of ALT (A and G) and HDL-C (B and H), as well as on the levels of hepatic lipids TG (C and I), TC (D and J), and FFA (E and K) and lipoperoxides (F and L) in MCD- and HFD-induced NASH mice, respectively. Values are the mean ± S.D. (n = 10/group). #$P < 0.05$; ##$P < 0.01$, compared with NC mice; *$P < 0.05$; **$P < 0.01$, compared with MCD or HFD mice.

above experimental mice were extracted, they were subjected to histochemical and histopathological examinations. H&E staining of liver tissues revealed remarkable hypertrophy of hepatocytes in MC mice of both MCD and HFD models compared with NC mice eating normal diets (Supplemental Fig. 1, A-b and C-b vs. Supplemental Fig. 1, A-a and C-a, respectively). Oil Red O staining of the liver tissues showed that the mice in both MC groups had severe steatohepatitis and a remarkable hepatic lipid accumulation compared with NC mice (Supplemental Fig. 1, B-b and D-b vs. Supplemental Fig. 1, B-a and D-a). In RSV treatment groups, neither MCD nor HFD mice showed significant histopathological improvement (Supplemental Fig. 1, A–D-c) compared with MC mice. In contrast, OCA and RLA8 treatments reversed both MCD- and HFD-induced NASH and could significantly lower the number and amount of fat droplets formed in the livers (Supplemental Fig. 1, A–D-d and A–D-e). It was also noticed that the number and size of inflammatory foci were significantly reduced in OCA- and RLA8-treated mice. Furthermore, the therapeutic efficacy of RLA8 was notably better than that of OCA. In fact, the morphologic looks of liver tissues from RLA8-treated mice were rather similar to those of normal mice (Supplemental Fig. 1, A–D-e vs. Supplemental Fig. 1, A–D-a).

To facilitate quantitative analysis and comparison of the results, we assigned to the tissues in each group an NAFLD activity score (NAS) according to the criteria listed in Table 1. Clearly, the NASs of mice in the RLA8 group for both NASH models (Table 3) were significantly lower than that of the MC group, a reduction of 53.1% and 60.2% ($P < 0.01$) for the MCD and HFD model, respectively. These results further corroborated that RLA8 could significantly improve liver injuries caused by NASH and its efficacy was slight better than OCA (NASs: 3.3 and 2.3 vs. 4.3 and 2.7).

To gain more insights into related pathology, we also performed biochemical analysis of the mice. In accordance

TABLE 3
The NASs for various groups of mice
Values are the mean ± S.D. (n = 10/group).

NAFLD	NC	MC	RSV	OCA	RLA8
MCD model	0.5 ± 0.5	7.1 ± 0.7*	5.7 ± 0.7**	4.3 ± 0.5***	3.3 ± 0.5***
HFD model	0.1 ± 0.3	5.9 ± 0.8*	4.2 ± 0.4**	2.7 ± 0.8***	2.3 ± 1.2***

*$P < 0.01$ vs. NC; **$P < 0.05$, ***$P < 0.01$ vs. MC.

with the observations above, we found that the contents of hepatic TG, TC, and FFA in MC mice of the MCD model increased by 8.75-fold, 4.30-fold, and 1.61-fold (Fig. 3C; Fig. 4, D and E), respectively, compared with those in NC mice, and they increased by 2.5-fold, 3.05-fold, and 1.43-fold in HFD MC mice (Fig. 3I; Fig. 4, J and K). Similarly, the hepatic lipoperoxide content in MC mice of both models also exhibited a significant increase (Fig. 3F; Fig. 4L). The accumulation of TG, TC, FFA, and lipoperoxide in mouse livers was associated with hepatic dysfunction, as revealed by the significantly elevated serum ALT levels for both models (Fig. 3, A and D).

The results in Fig. 3, C–E and I–K further showed that RLA8 treatment could reverse hepatic lipid accumulation in both NASH models. Compared with MC mice, hepatic TG, TC, and FFA contents in RLA8-treated mice were reduced by 61.1%, 40.1%, and 38.4% in the MCD model and by 34.8%, 52.2%, and 29.2% in the HFD model, respectively. OCA treatment gave similar results, but it reduced hepatic TG, TC, and FFA contents by only 21.3%, 28.4%, and 7.9% in the MCD model, and by 14.9%, 34.7%, and 20.4% in the HFD model, which were much less impressive values than the reductions induced by RLA8. On the other hand, RSV could only marginally reduce FFA accumulation and had no significant impact on hepatic TG and TC contents. Moreover, RLA8 treatment significantly increased the HDL-C content (Fig. 3, B and F) ($P < 0.01$), but OCA and RSV did not have any obvious effect. Although RSV treatment had no significant influence on hepatic TG and TC contents, it could reverse the lipoperoxide content of NASH mice to the normal level, just like RLA8 and OCA. In addition, all three compounds were able to restore hepatic functions in NASH mice, as indicated by the recovered serum ALT levels after treatments (Fig. 3, A and G). Again, RLA8 seemed to be more potent than OCA and RSV in this respect. These results agreed very well with that of above histochemical and histopathological studies, which indicated that RLA8 was more potent than OCA, which was then much more potent than RSV, to reverse hepatic lipid accumulation and steatohepatitis in both disease models.

The Influence of RLA8 Treatment on Hepatic Inflammation Associated with NASH. NASH usually is accompanied in patients by metabolic inflammation featuring elevated levels of C-reactive proteins and various ILs (Jiang et al., 2016). Inconsistent with these observations, we also noticed an elevated level of inflammatory activities in the MCD and HFD mice, including an increased number of inflammatory cells (Supplemental Fig. 1, A and C-b) and elevated levels of major hepatic inflammation markers, such as TNF-α, IL-6, and IL-10 (Fig. 4). It was revealed that RSV, OCA, and RLA8 could all reduce NASH-induced TNF-α, IL-6, and IL-10 secretion (Fig. 4) and, consequently, alleviate related hepatic inflammation. Again, RLA8 showed more potent therapeutic efficacy than RSV and OCA, especially in the more severe MCD NASH model (Fig. 4, A–C).

The Influence of RLA8 Treatment on Hepatic Fibrosis in MCD-Induced NASH Mice. Hepatic fibrosis is triggered by chronic injuries, especially inflammation, and represents one of the common and severe concerns in NASH, since it can lead to portal hypertension and cirrhosis to disrupt hepatic function. Therefore, we also examined the impact of RLA8 treatment on hepatic fibrosis based on liver biopsy samples. In this regard, the liver sections from MCD and NC mice were stained with trichrome and then subjected to histopathological

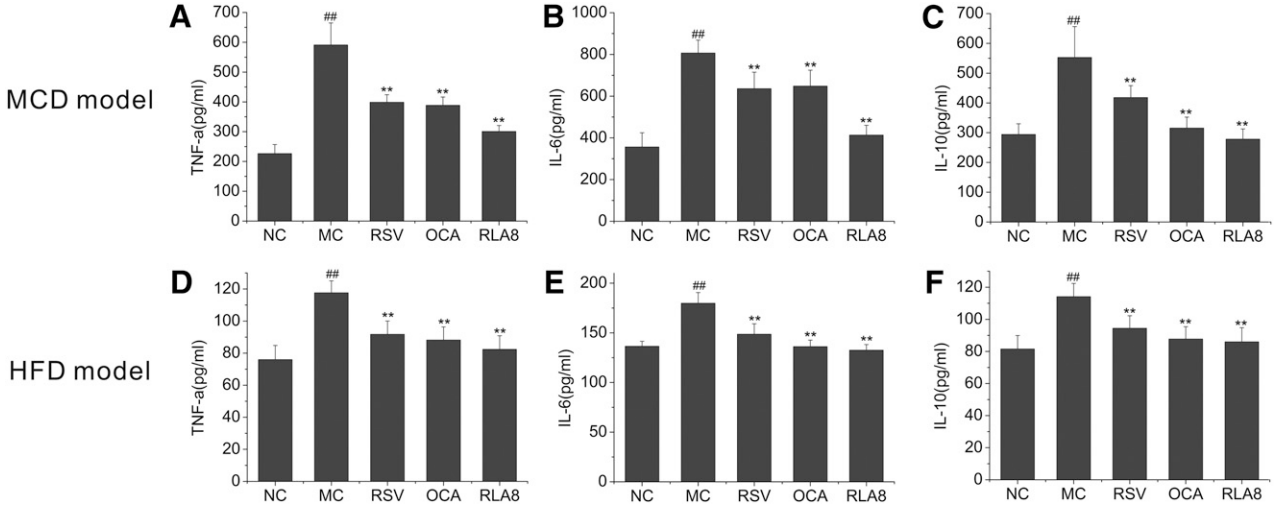

Fig. 4. The influences of RSV, OCA and RLA8 treatments on the secretion levels of major hepatic inflammation markers TNF-α A and D, IL-6 B and E, and IL-10 C and F in MCD and HFD NASH mice. Values are the mean ± S.D. (n = 10/group). ##$P < 0.01$, compared with NC mice; **$P < 0.01$, compared with MCD or HFD mice.

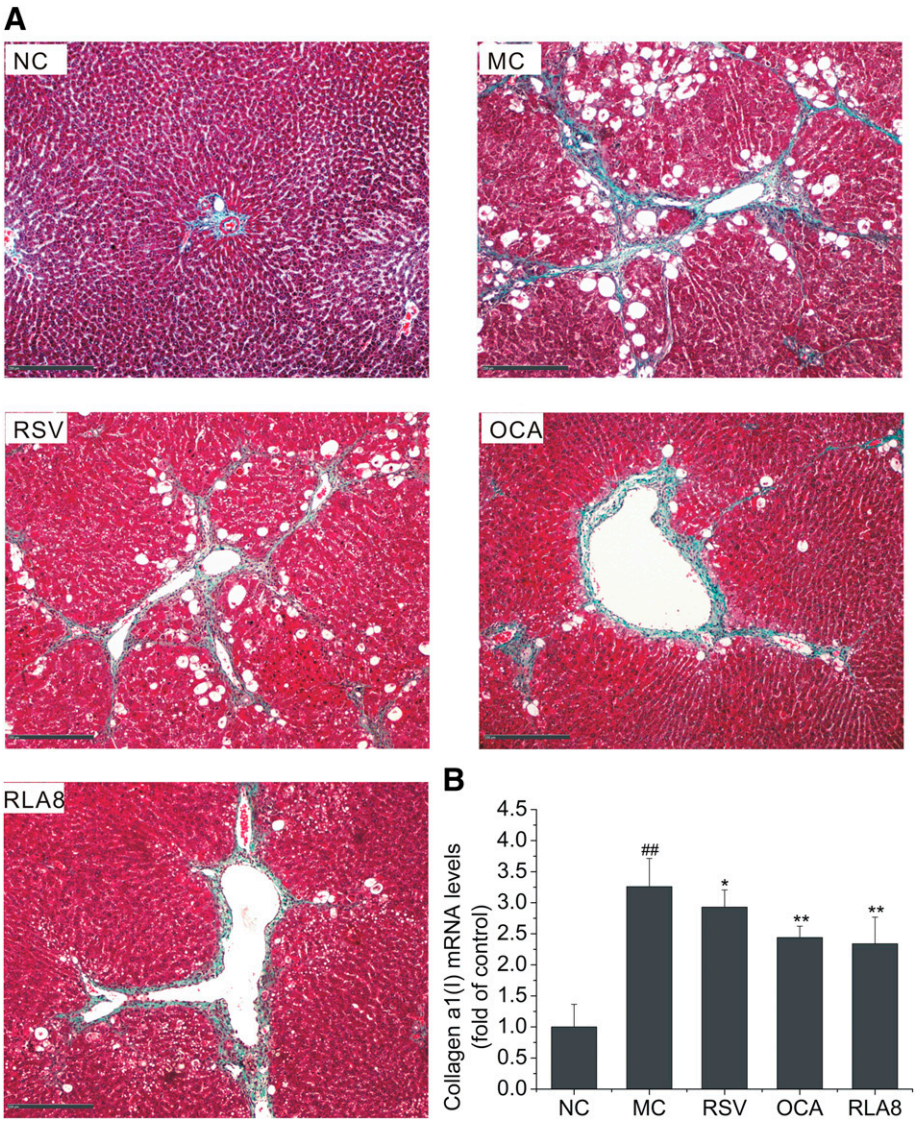

Fig. 5. The influences of RSV, OCA, and RLA8 treatments on hepatic fibrosis in MCD NASH mice. (A) Representative photomicrographs (original magnification, 100×; scale bar, 250 μm) of livers from mice of the NC, MC, MCD + RSV (100 mg/kg); MCD + OCA (10 mg/kg); and MCD + RLA8 (100 mg/kg) groups, with liver sections stained with trichrome and pericellular fibrosis indicated by arrows. (B) Hepatic mRNA expression of collagen α1(I) assessed using reverse-transcription PCR with values (mean ± S.D.) normalized against the internal control GAPDH. ##$P < 0.01$ compared with NC; *$P < 0.05$; **$P < 0.01$ compared with MC.

examination. In line with previous reports, a lack of the essential amino acid methionine and choline in the MCD diet promoted severe steatohepatitis and the occurrence of appreciable hepatic sinusoidal fibrosis. Evidently, RSV, OCA, and RLA8 treatments could all alleviate hepatic fibrosis (Fig. 5A). In particular, OCA and RLA8 treatments could reverse hepatic fibrosis almost completely. In agreement with this discovery, elevated expression of the hepatic collagen α1 gene (Fig. 5B) in MCD mice was effectively suppressed by all three compounds.

The Influence of RLA8 Treatment on Insulin Resistance Associated with HFD-Induced NASH. Insulin resistance is another important hallmark for NAFLD (Cusi et al., 2016). However, MCD does not cause insulin resistance, although it can induce a more severe form of NASH and fibrosis in mice. In contrast, HFD can induce mild peripheral insulin resistance, as reflected by significantly increased serum levels of glucose, insulin, TG, and TC, as well as HOMA-IR, in HFD MC mice (Fig. 6). Consequently, we examined the impacts of RSV, OCA, and RLA8 treatments on insulin resistance associated with the HFD model. It was found that all three compounds led to a significant reduction in serum glucose and insulin levels and HOMA-IR (Fig. 6, A, B, and E), suggesting great improvement in insulin resistance in these mice. This was associated with the significant improvement of HFD-induced hyperlipidemia, namely, elevated serum TG and TC levels, in the case of OCA and RLA8 ($P < 0.05$), although changes in serum TG and TC levels in the RSV group were not so obvious (Fig. 6, C and D).

The Influence of RLA8 Treatment on the Expression of Genes and Proteins Associated with NASH. To help elucidate the underlying mechanism by which RLA8 improves NASH in MCD mice, we analyzed the expression level of PPAR-related genes and proteins involved in hepatic lipid metabolism, inflammation, and fibrosis by PCR and Western blot. The expression of genes and proteins regulating lipid synthesis, including SREBP1, FAS, and SCD1, or inflammation and fibrosis, including VCAM1, TIMP1, and TGFβ1, were dramatically upregulated in MC mice, compared with NC mice (Fig. 7, A–C). RLA8 treatment was found to significantly suppress the expression of all assessed genes and proteins, except for TGFβ1. These results suggested that RLA8-induced reduction in hepatic lipid accumulation, inflammation, and fibrosis was coupled with reduced expression of the downstream hepatic genes and proteins of PPARs (Fig. 7D).

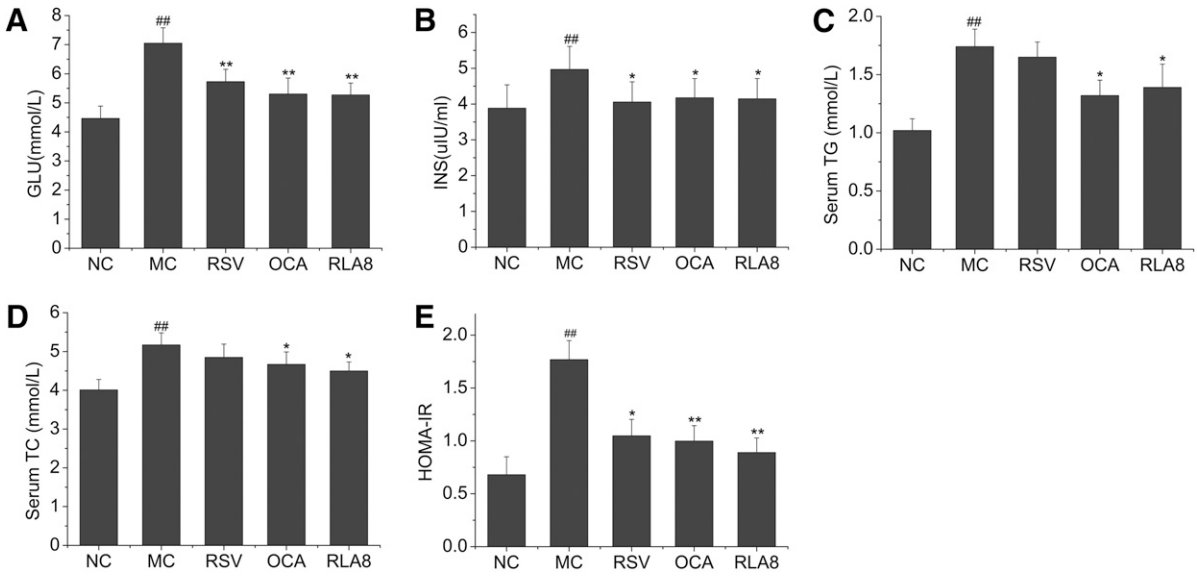

Fig. 6. The impacts of RSV, OCA, and RLA8 treatments on insulin resistance in HFD NASH mice, reflected by serum glucose (A), insulin (B), TG (C), and TC levels (D), as well as HOMA-IR (E). Values are the mean ± S.D. (n = 10/group). ##$P < 0.01$ compared with NC; *$P < 0.05$; **$P < 0.01$, compared with MC.

Considering that SREBP1, FAS, and SCD1 expression is regulated by the AMPK-ACC pathway and that the AMPK-ACC pathway is closely related to fatty acid biosynthesis and lipogenesis (Rhee, 2001; Hawley et al., 2005; Shapiro et al., 2005; Li et al., 2011), we then assessed the AMPK activity by measuring Thr172 phosphorylation of AMPKα and its major downstream protein p-ACC (Ser79), as AMPK activation can lead to the phosphorylation and inhibition of ACC, which is the rate-limiting enzyme in fatty acid biosynthesis (Weltman et al., 1998; Tong, 2005). Western blot results (Fig. 7, E and F) disclosed that, compared with the MC group, RLA8 treatment could significantly enhance the phosphorylation of AMPKα and ACC.

Discussion

PPAR has three subtypes, PPAR-α, PPAR-δ, and PPAR-γ, and its activation has been demonstrated to improve NAFLD and NASH primarily via suppressing lipogenesis and enhancing β-oxidation–associated hepatic fatty acid disposal (Cottart et al., 2014; Pawlak et al., 2014). Employing balanced pan-PPAR agonists to treat NAFLD and NASH may have additional significant advantages, such as synergetic therapeutic efficacy, and thus has become an attractive direction (Tenenbaum and Fisman, 2012). In previous studies (Xu and Xie, 2009; Chen et al., 2014), we have developed a pan-PPAR agonist, ZBH, by combining the pharmacophores of fibrates and RSV. ZBH had exhibited relatively balanced agonist activity in vitro for all three PPAR subtypes and was more potent than fenofibric acid in vivo in reducing TG accumulation (Chen et al., 2014). These discoveries led us to design a completely novel type of multitargeting agonist that contained not only the key structural and pharmacophore motifs of pan-PPAR agonists but also the structural motif of GPR40 agonists (i.e., a long chain fatty acid moiety) (Briscoe et al., 2003), as GPR40 is also an important target for the treatment of hepatic steatosis. The current study has verified that the compound RLA8, which was developed on the basis of this new drug design principle, was a potent and balanced quadruple agonist for PPAR-α, PPAR-δ, PPAR-γ, and GPR40, with the EC_{50} values all in the low-micromolar range. And the off-target effect assays of RLA8 toward FXR and GPBAR1 showed that the maximum response of RLA8 to both receptors was less than 10% (Supplemental Fig. 2). Most significantly, detailed in vivo studies on RLA8 have revealed its great efficacy to improve all of the symptoms related to NAFLD and NASH.

The therapeutic efficacy of RLA8 compared with NASH was evaluated in mice using two NASH models induced by HFD and MCD diets, respectively, which represent different severities of the disease, and were compared with two positive reference drugs, RSV and OCA. Abnormal body weight change is one of the important NASH parameters for these disease models. It was shown that RLA8 treatment could completely prevent MCD-caused mouse body weight loss (Fig. 2A) and reverse in a time-dependent manner the trend of body weight gains in HFD mice (Fig. 2C), and that its efficacy was significantly better than those of both reference drugs.

Histochemical and hepatic histopathological studies of the experimental mice have disclosed that RLA8 and OCA treatments could reverse the number and size of fat droplets and inflammation foci in both MCD and HFD models (Supplemental Fig. 1), and could significantly alleviate hepatic fibrosis (Fig. 5A) that can only be created in the more severe MCD model. This observation was further corroborated by biochemical analysis results showing significant decreases of TG, TC, FFA, and lipoperoxide contents related to hepatic lipid accumulation (Fig. 3, C–F and I–L), and of hepatic inflammation-related key markers, such as TNF-α, IL-6, and IL-10 (Fig. 3, A–F), in RLA8 and OCA-treated mice for both NASH models; significant decreases of hepatic mRNA expression of liver fibrosis-related collagen α1(I) in RLA8 and OCA-treated MCD mice (Fig. 5B); and much improved insulin resistance in RLA8 and OCA-treated HFD mice (Fig. 6E). These pathologic and biochemical changes were associated with the improvement of liver injury and the restoration of hepatic function, as reflected by the significantly reduced

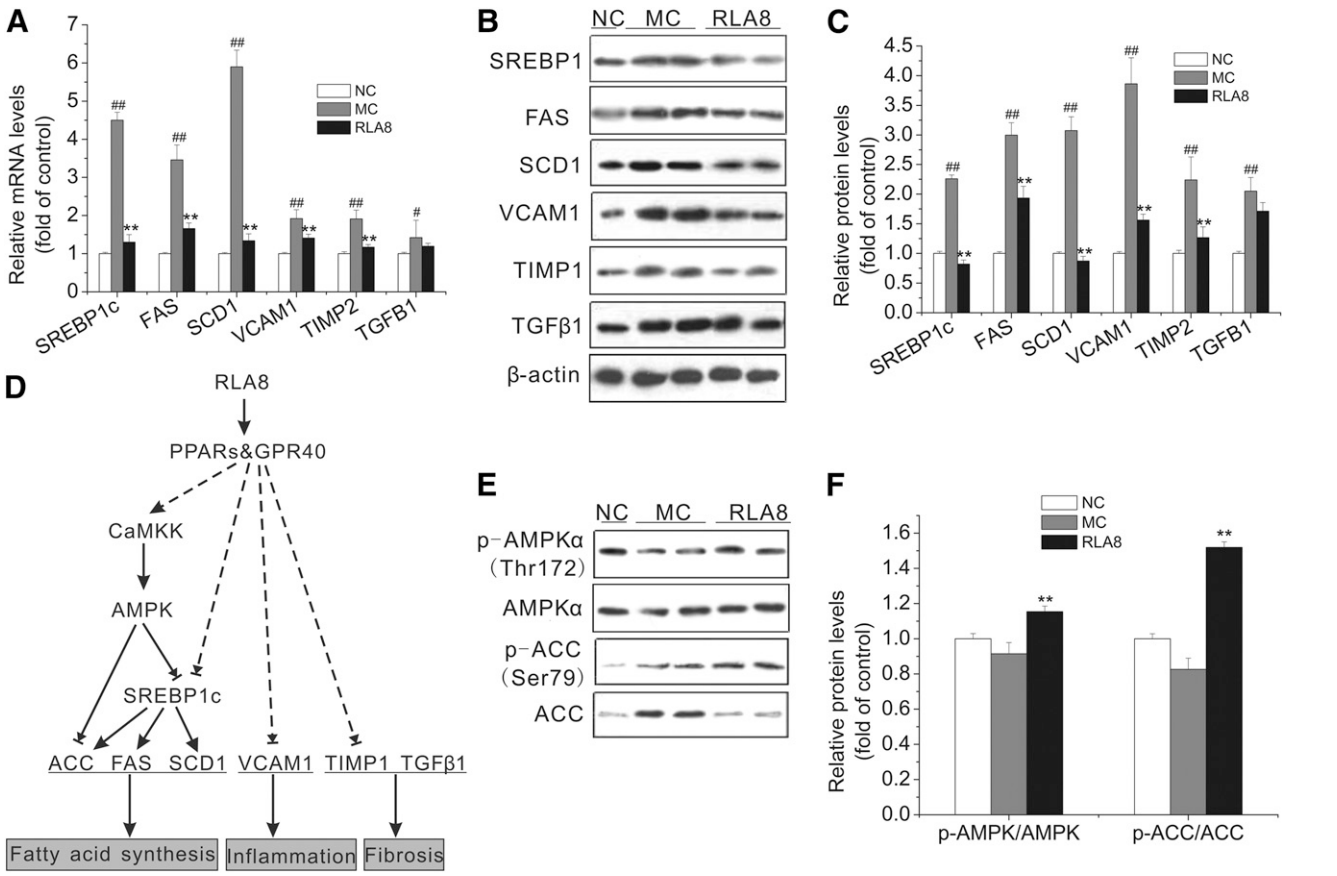

Fig. 7. The influence of RLA8 treatment on the expression of proteins related to hepatic lipogenesis and fibrogenesis and the AMPK pathway in MCD mice. (A) Hepatic mRNA levels of target genes assessed using reverse-transcription PCR with values normalized against an internal control, GAPDH. Western blot results of hepatic lipogenesis and fibrogenesis-related proteins (B) and their densitometric quantification (C). (D) Proposed mechanisms for RLA8 to participate in reversing MCD-induced NASH. Western blot results of phosphorylated AMPKα and ACC (E) and their densitometric quantification (F). Values are given as the mean ± S.D. expressed in fold changes compared with NC. #$P < 0.05$; ##$P < 0.01$ compared with NC; **$P <$ 0.01 compared MCD mice.

serum levels of ALT (Fig. 3, A and G). In most cases, RSV had similar beneficial effects against NASH, but it was much less effective than RLA8 and OCA. Most significantly, RLA8 showed almost uniformly better efficacy than OCA for all parameters examined. In fact, the overall NAS (Table 3) of mice in the RLA8 group for both MCD (NAS, 3.3) and HFD (NAS 2.3) models were nearly none-NASH (NAS, <3.0), and the morphologic looks of their liver tissues were very similar to those of normal mice (Fig. 5; Supplemental Fig. 1e). Another beneficial effect associated with RLA8 treatment was the significantly increased levels of serum HDL-C, the "good cholesterol," in both MCD and HFD models (Fig. 3, B and H), and this was not observed with OCA and RSV treatments.

Hepatic and peripheral insulin resistance is a general feature of NASH, and it is usually associated with lipotoxicity and hepatic inflammation. Moreover, hyperlipidemia (i.e., elevated concentrations of plasma lipids) and increased production of proinflammatory cytokines also contribute to or exacerbate hepatic inflammation and fibrosis further. The improvement of all these parameters, including insulin resistance, hyperlipidemia, and proinflammatory cytokine production, upon treatment with RLA8 may be the explanation for its great efficacy in alleviating NASH-related hepatic inflammation, fibrosis, and other symptoms observed with both NASH models.

Detailed biochemical analysis of the expression levels of genes/proteins related to lipogenesis and fibrogenesis, including SREBP1, FAS, SCD1, VCAM1, TIMP1, TGFβ1 (Fig. 7, B and C), and collagen α1(I) (Fig. 5B), all of which were drastically upregulated in MCD mice, provided additional insight into the action mechanism of RLA8. It was shown that RLA8 treatment could downregulate the expression of all these proteins, except for TGFβ1, at mRNA and/or protein levels. As the expression of SREBP1, FAS, and SCD1 is regulated by the AMPK-ACC pathway, we also assessed the AMPK activity and its major downstream protein ACC to discover that RLA8 could significantly enhance the phosphorylation of AMPKα and ACC. AMPK is a heterotrimeric kinase, composed of a conserved catalytic α subunit and two regulatory subunits, β and γ. The kinase activity of its α subunit can be increased by two to three orders of magnitude upon Thr172 phosphorylation of its activation loop (Hawley et al., 1996). AMPK phosphorylates ACC Ser79 to lead to its inactivation, whereas ACC is the rate-limiting enzyme in fatty acid synthesis (Weltman et al., 1998; Tong, 2005). AMPK activation also reduces the expression of SREBP-1, a lipogenic transcription factor that can suppress lipogenesis (Li et al., 2011). In turn, AMPK phosphorylation is realized by the Ca^{2+}/calmodulin-dependent protein kinase CaMKKβ (Hawley et al., 2005). GPR40 is a Gαq/11-coupled receptor, which activates phospholipase C

(Rhee, 2001) to elevate the intracellular Ca^{2+} concentration (Shapiro et al., 2005).

TGFβ1 is an important profibrogenic cytokine that favors extracellular matrix deposition. Increased levels of TGFβ1 have been detected in human fibrotic livers and in the livers of rats fed with the MCD diet (George et al., 2003); thus, it is likely to play a role in the development of hepatic fibrosis. However, RLA8 did not have a significant impact on the expression level of TGFβ1, indicating that RLA8 reversed fibrosis, probably through the reduction of liver lipids such as TGs and lipoperoxides, which are known to regulate collagen I gene expression, rather than through inhibiting profibrogenic cytokine expression. In accordance with this, RLA8 was found to substantially improve HFD-induced insulin resistance and hyperlipidemia.

Based on the above evidence and also on literature results, we have proposed in Fig. 7D an action mechanism for RLA8. As a pan-PPAR and GPR40 agonist, RLA8 might induce AMPK activation to result in ACC inactivation and downregulation of SREBP1, FAS, and SCD1 expression to reduce lipid synthesis, so as to prevent hepatic lipid accumulation and thereby related inflammation and fibrosis. In the meantime, PPAR-$\alpha/\gamma/\delta$ and GPR40 activation by RLA8 might also directly lead to downregulated expression of proinflammatory and profibrogenic proteins (e.g., VCAM1, TIMP1, and hepatic collagen α1) to further suppress hepatic inflammation and fibrosis.

In conclusion, we have introduced in this work a completely new class of anti-NASH drugs, such as RLA8. It was proved to be a balanced quadruple agonist for PPAR-$\alpha/\gamma/\delta$ and GPR40 and exhibited a superb efficacy to reverse NASH-induced hepatic lipid accumulation, steatosis, inflammation, fibrosis, and other damage associated with both HFD-induced mild and MCD-induced severe mouse NASH models. Most impressively, RLA8 showed a significantly better efficacy to treat NASH than reference "drugs" RSV and OCA, whereas currently OCA is the most promising NASH drug candidate that is in phase III clinical trials and there has been no clinically approved drug to treat NASH yet. Compared with some subtype-selective PPAR agonists, such as PPAR-α/δ agonist elafibranor (EC_{50} = 45–175 nM) (Cariou and Staels, 2014) or specific GPR40 agonist GW9508 (EC_{50} = 50 nM) (Briscoe et al., 2006), the agonist activities of RLA8 in each individual acceptor (EC_{50} = 1–28 μM) may not seem to be extremely potent, but the overall therapeutic efficacy of RLA8 was way superior to all compounds reported thus far. This may be explained by the synergetic effects upon balanced inhibition of multiple hepatic lipogenesis, inflammation, and fibrogenesis-related receptor targets by RLA8, as this can prevent compensatory responses through alternative pathways. In addition, our preliminary studies also showed that RLA8 had fewer and less severe side effects than the reference drugs. Therefore, RLA8 represents a new NASH drug candidate worthy of further investigation, and we are now in the process of pushing it toward clinical studies.

Authorship Contributions

Participated in research design: Li, Wei guo Shi, Zhong, and Guo.

Conducted experiments: Li, Chen, Sun, and Zhou.

Contributed new reagents or analytic tools: Chen, Li li Wang, Yu cong Shi and Chu han Wang.

Performed data analysis: Li, Chen, Wei guo Shi, and Guo.

Wrote or contributed to the writing of the manuscript: Li, Chen, Li li Wang, and Guo.

References

Adams LA, Lymp JF, St Sauver J, Sanderson SO, Lindor KD, Feldstein A, and Angulo P (2005) The natural history of nonalcoholic fatty liver disease: a population-based cohort study. *Gastroenterology* **129**:113–121.

Briscoe CP, Peat AJ, McKeown SC, Corbett DF, Goetz AS, Littleton TR, McCoy DC, Kenakin TP, Andrews JL, Ammala C, et al. (2006) Pharmacological regulation of insulin secretion in MIN6 cells through the fatty acid receptor GPR40: identification of agonist and antagonist small molecules. *Br J Pharmacol* **148**:619–628.

Briscoe CP, Tadayyon M, Andrews JL, Benson WG, Chambers JK, Eilert MM, Ellis C, Elshourbagy NA, Goetz AS, Minnick DT, et al. (2003) The orphan G protein-coupled receptor GPR40 is activated by medium and long chain fatty acids. *J Biol Chem* **278**:11303–11311.

Cariou B, Hanf R, Lambert-Porcheron S, Zaïr Y, Sauvinet V, Noël B, Flet L, Vidal H, Staels B, and Laville M (2013) Dual peroxisome proliferator-activated receptor α/δ agonist GFT505 improves hepatic and peripheral insulin sensitivity in abdominally obese subjects. *Diabetes Care* **36**:2923–2930.

Cariou B and Staels B (2014) GFT505 for the treatment of nonalcoholic steatohepatitis and type 2 diabetes. *Expert Opin Investig Drugs* **23**:1441–1448.

Cavallaro A, Ainis T, Bottari C, and Fimiani V (2003) Effect of resveratrol on some activities of isolated and in whole blood human neutrophils. *Physiol Res* **52**: 555–562.

Chalasani N, Younossi Z, Lavine JE, Diehl AM, Brunt EM, Cusi K, Charlton M, and Sanyal AJ (2012) The diagnosis and management of non-alcoholic fatty liver disease: practice Guideline by the American Association for the Study of Liver Diseases, American College of Gastroenterology, and the American Gastroenterological Association. *Hepatology* **55**:2005–2023.

Chen W, Fan S, Xie X, Xue N, Jin X, and Wang L (2014) Novel PPAR pan agonist, ZBH ameliorates hyperlipidemia and insulin resistance in high fat diet induced hyperlipidemic hamster. *PLoS One* **9**:e96056.

Cottart CH, Nivet-Antoine V, and Beaudeux JL (2014) Review of recent data on the metabolism, biological effects, and toxicity of resveratrol in humans. *Mol Nutr Food Res* **58**:7–21.

Cusi K (2016) Treatment of patients with type 2 diabetes and non-alcoholic fatty liver disease: current approaches and future directions. *Diabetologia* **59**:1112–1120.

Ekstedt M, Franzén LE, Mathiesen UL, Thorelius L, Holmqvist M, Bodemar G, and Kechagias S (2006) Long-term follow-up of patients with NAFLD and elevated liver enzymes. *Hepatology* **44**:865–873.

Gao X, Fu T, Wang C, Ning C, Liu K, Liu Z, Sun H, Ma X, Huo X, Yang X, et al. (2018) Yangonin protects against cholestasis and hepatotoxity via activation of farnesoid X receptor in vivo and in vitro. *Toxicol Appl Pharmacol* **348**:105–116.

Gawrieh S and Chalasani N (2018) Emerging treatments for nonalcoholic fatty Liver disease and nonalcoholic Steatohepatitis. *Clin Liver Dis* **22**:189–199.

George J, Pera N, Phung N, Leclercq I, Yun Hou J, and Farrell G (2003) Lipid peroxidation, stellate cell activation and hepatic fibrogenesis in a rat model of chronic steatohepatitis. *J Hepatol* **39**:756–764.

Hansen HH, Feigh M, Veidal SS, Rigbolt KT, Vrang N, and Fosgerau K (2017) Mouse models of nonalcoholic steatohepatitis in preclinical drug development. *Drug Discov Today* **22**:1707–1718.

Hawley SA, Davison M, Woods A, Davies SP, Beri RK, Carling D, and Hardie DG (1996) Characterization of the AMP-activated protein kinase kinase from rat liver and identification of threonine 172 as the major site at which it phosphorylates AMP-activated protein kinase. *J Biol Chem* **271**:27879–27887.

Hawley SA, Pan DA, Mustard KJ, Ross L, Bain J, Edelman AM, Frenguelli BG, and Hardie DG (2005) Calmodulin-dependent protein kinase kinase-β is an alternative upstream kinase for AMP-activated protein kinase. *Cell Metab* **2**:9–19.

Heebøll S, Thomsen KL, Clouston A, Sundelin EI, Radko Y, Christensen LP, Ramezani-Moghadam M, Kreutzfeldt M, Pedersen SB, Jessen N, et al. (2015) Effect of resveratrol on experimental non-alcoholic steatohepatitis. *Pharmacol Res* **95–96**:34–41.

Jiang ZG, de Boer IH, Mackey RH, Jensen MK, Lai M, Robson SC, Tracy R, Kuller LH, and Mukamal KJ (2016) Associations of insulin resistance, inflammation and liver synthetic function with very low-density lipoprotein: the Cardiovascular Health Study. *Metabolism* **65**:92–99.

Kleiner DE, Brunt EM, Van Natta M, Behling C, Contos MJ, Cummings OW, Ferrell LD, Liu YC, Torbenson MS, Unalp-Arida A, et al.; Nonalcoholic Steatohepatitis Clinical Research Network (2005) Design and validation of a histological scoring system for nonalcoholic fatty liver disease. *Hepatology* **41**:1313–1321.

Lau JKC, Zhang X, and Yu J (2017) Animal models of non-alcoholic fatty liver disease: current perspectives and recent advances. *J Pathol* **241**:36–44.

Li M, Zhou X, Mei J, Geng X, Zhou Y, Zhang W, and Xu C (2014) Study on the activity of the signaling pathways regulating hepatocytes from G0 phase into G1 phase during rat liver regeneration. *Cell Mol Biol Lett* **19**:181–200.

Li W, Jia HY, He XH, Shi WG, and Zhong BH (2012) Novel phenoxyalkylcarboxylic acid derivatives as hypolipidaemic agents. *J Enzyme Inhib Med Chem* **27**:311–318.

Li X and Kazgan N (2011) Mammalian sirtuins and energy metabolism. *Int J Biol Sci* **7**:575–587.

Li Y, Xu S, Mihaylova MM, Zheng B, Hou X, Jiang B, Park O, Luo Z, Lefai E, Shyy JY, et al. (2011) AMPK phosphorylates and inhibits SREBP activity to attenuate hepatic steatosis and atherosclerosis in diet-induced insulin-resistant mice. *Cell Metab* **13**:376–388.

Machado MV, Michelotti GA, Xie G, de Almeida TP, Boursier J, Bohnic B, Guy CD, and Diehl AM (2015) Correction: mouse models of diet-induced nonalcoholic steatohepatitis reproduce the heterogeneity of the human disease. *PLoS One* **10**: e0132315.

Marin V, Rosso N, Dal Ben M, Raseni A, Boschelle M, Degrassi C, Nemeckova I, Nachtigal P, Avellini C, Tiribelli C, et al. (2016) An animal model for the juvenile

non-alcoholic fatty liver disease and non-alcoholic steatohepatitis. *PLoS One* **11**: e0158817.
Markham A and Keam SJ (2016) Obeticholic acid: first global approval. *Drugs* **76**: 1221–1226.
Matthews DR, Hosker JP, Rudenski AS, Naylor BA, Treacher DF, and Turner RC (1985) Homeostasis model assessment: insulin resistance and β-cell function from fasting plasma glucose and insulin concentrations in man. *Diabetologia* **28**: 412–419.
Nakata R, Takahashi S, and Inoue H (2012) Recent advances in the study on resveratrol. *Biol Pharm Bull* **35**:273–279.
Neuschwander-Tetri BA, Loomba R, Sanyal AJ, Lavine JE, Van Natta ML, Abdelmalek MF, Chalasani N, Dasarathy S, Diehl AM, Hameed B, et al.; NASH Clinical Research Network (2015) Farnesoid X nuclear receptor ligand obeticholic acid for non-cirrhotic, non-alcoholic steatohepatitis (FLINT): a multicentre, randomised, placebo-controlled trial. *Lancet* **385**:956–965.
Ou HY, Wu HT, Hung HC, Yang YC, Wu JS, and Chang CJ (2013) Multiple mechanisms of GW-9508, a selective G protein-coupled receptor 40 agonist, in the regulation of glucose homeostasis and insulin sensitivity. *Am J Physiol Endocrinol Metab* **304**:E668–E676.
Ou HY, Wu HT, Lu FH, Su YC, Hung HC, Wu JS, Yang YC, Wu CL, and Chang CJ (2014) Activation of free fatty acid receptor 1 improves hepatic steatosis through a p38-dependent pathway. *J Mol Endocrinol* **53**:165–174.
Pawlak M, Baugé E, Bourguet W, De Bosscher K, Lalloyer F, Tailleux A, Lebherz C, Lefebvre P, and Staels B (2014) The transrepressive activity of peroxisome proliferator-activated receptor alpha is necessary and sufficient to prevent liver fibrosis in mice. *Hepatology* **60**:1593–1606.
Pellicciari R, Fiorucci S, Camaioni E, Clerici C, Costantino G, Maloney PR, Morelli A, Parks DJ, and Willson TM (2002) 6α-ethyl-chenodeoxycholic acid (6-ECDCA), a potent and selective FXR agonist endowed with anticholestatic activity. *J Med Chem* **45**:3569–3572.
Ratziu V, Harrison SA, Francque S, Bedossa P, Lehert P, Serfaty L, Gomez MR, Boursier J, Abdelmalek M, Caldwell S, et al. (2016) Elafibranor, an agonist of the peroxisome proliferator-activated receptor-α and-δ, induces resolution of nonalcoholic steatohepatitis without fibrosis worsening. *Gastroenterology* **150**:1147–1159.e5.
Rhee SG (2001) Regulation of phosphoinositide-specific phospholipase C. *Annu Rev Biochem* **70**:281–312.
Rodrigues PM, Afonso MB, Simão AL, Carvalho CC, Trindade A, Duarte A, Borralho PM, Machado MV, Cortez-Pinto H, Rodrigues CM, et al. (2017) miR-21 ablation and obeticholic acid ameliorate nonalcoholic steatohepatitis in mice. *Cell Death Dis* **8**:e2748.
Shapiro H, Shachar S, Sekler I, Hershfinkel M, and Walker MD (2005) Role of GPR40 in fatty acid action on the β cell line INS-1E. *Biochem Biophys Res Commun* **335**: 97–104.
Suh HN, Huong HT, Song CH, Lee JH, and Han HJ (2008) Linoleic acid stimulates gluconeogenesis via Ca2+/PLC, cPLA2, and PPAR pathways through GPR40 in primary cultured chicken hepatocytes. *Am J Physiol Cell Physiol* **295**: C1518–C1527.
Tenenbaum A and Fisman EZ (2012) Balanced pan-PPAR activator bezafibrate in combination with statin: comprehensive lipids control and diabetes prevention? *Cardiovasc Diabetol* **11**:140.
Tong L (2005) Acetyl-coenzyme A carboxylase: crucial metabolic enzyme and attractive target for drug discovery. *Cell Mol Life Sci* **62**:1784–1803.
Towbin H, Staehelin T, and Gordon J (1979) Electrophoretic transfer of proteins from polyacrylamide gels to nitrocellulose sheets: procedure and some applications. *Proc Natl Acad Sci USA* **76**:4350–4354.
Vernon G, Baranova A, and Younossi ZM (2011) Systematic review: the epidemiology and natural history of non-alcoholic fatty liver disease and non-alcoholic steatohepatitis in adults. *Aliment Pharmacol Ther* **34**:274–285.
Weltman MD, Farrell GC, Hall P, Ingelman-Sundberg M, and Liddle C (1998) Hepatic cytochrome P450 2E1 is increased in patients with nonalcoholic steatohepatitis. *Hepatology* **27**:128–133.
Weltman MD, Farrell GC, and Liddle C (1996) Increased hepatocyte CYP2E1 expression in a rat nutritional model of hepatic steatosis with inflammation. *Gastroenterology* **111**:1645–1653.
Williams CD, Stengel J, Asike MI, Torres DM, Shaw J, Contreras M, Landt CL, and Harrison SA (2011) Prevalence of nonalcoholic fatty liver disease and nonalcoholic steatohepatitis among a largely middle-aged population utilizing ultrasound and liver biopsy: a prospective study. *Gastroenterology* **140**: 124–131.
Xu Y and Xie X (2009) Glucagon receptor mediates calcium signaling by coupling to G alpha q/11 and G alpha i/o in HEK293 cells. *J Recept Signal Transduct Res* **29**: 318–325.

Address correspondence to: Dr. Zhong Wu Guo, Shandong University, 27 Shanda Nan Lu, Jinan 250100, People's Republic of China. E-mail: zwguo@sdu.edu.cn; or Dr. Wei Guo Shi, Beijing Institute of Pharmacology and Toxicology, 27 Tai-Ping Road, Beijing 100850, People's Republic of China. E-mail: shiwg1988@126.com

Journal of Pharmacology and Experimental Therapeutics

RLA8 - A new and highly effective quadruple PPARs-α/γ/δ and GPR40 agonist to reverse nonalcoholic steatohepatitis and fibrosis

Meng Hua Li, Wei Chen, Li Li Wang, Jia Lin Sun, Lei Zhou, Yu Cong Shi, Chu Han Wang, Bo Hua Zhong, Wei Guo Shi, Zhong Wu Guo

Supplemental Table 1. Primer sequences used for real time PCR reactions

Target	Sequences
GAPDH	F: GAGCCAAAAGGGTCATCATCT
	R: AGGGGCCATCCACAGTCTTC
Col1a1	F: GCACGAGTCACACCGGAAC
	R: CCAATGTCCAAGGGAGCCAC
SREBP-1c	F: GGAGGGGTAGGGCCAACGGCCT
	R: CATGTCTTCGAAAGTGCAATCAC
FAS	F: TCCTGCCTCTGGTGCTTGCT
	R: AGTTTCACGAACCCGCCTCCT
SCD1	F: CGAGAGTCAGGAGGGCAGGTTT
	R: TGATGGTGGTGGTGGTCGTGTA
Vcam1	F: AGTGTTGCTTGGACTGACTGTTG
	R: TGACCTCTTTACCGTTTGCCTAT
Timp1	F: TCCCAGAACCGCAGTGAAG
	R: TCAGAGCCCACGAGGACC
TGF-β1	F: ACAACGCCATCTATGAGAAAACC
	R: GCAGCTCTGCACGGGACA

Supplemental Table 2-1. The influences of RLA8, RSV, and OCA on the body weight change and food intake in MCD -induced NASH mice.

Body weight (g)					
week	NC	MC	RSV	OCA	RLA8
1	24.3±0.30	25.66±0.33			
2	24.63±0.25	25.58±0.23			
3	25.43±0.33	21.07±0.21			
4	26.22±0.23	19.01±0.23			
5	26.97±0.22	16.94±0.30			
6	27.68±0.23	16.58±0.33	17.01±0.33	17.05±0.32	17.08±0.33
7	27.67±0.31	15.63±0.23$^{\#\#}$	16.72±0.23	16.1±0.23	17.07±0.23**
8	27.23±0.25	15.14±0.21$^{\#\#}$	16.01±0.21	15.46±0.21	16.94±0.22**
9	27.33±0.32	14.47±0.25$^{\#\#}$	15.51±0.25	15.16±0.32	16.84±0.23**

Food intake (g)					
week	NC	MC	RSV	OCA	RLA8
1	3.45±0.10	2.71±0.13			
2	4.29±0.15	1.97±0.12			
3	4.22±0.13	1.86±0.12			
4	4.07±0.12	1.78±0.12			
5	4.06±0.12	1.61±0.13			
6	3.93±0.11	1.48±0.13	1.45±0.13	1.43±0.11	1.46±0.13
7	3.71±0.13	1.26±0.12	1.31±0.12	1.20±0.12	1.45±0.12
8	3.70±0.12	1.24±0.12	1.14±0.12	1.11±0.12	1.45±0.12
9	3.67±0.13	1.22±0.12	1.06±0.13	1.07±0.13	1.45±0.12

Values are the mean ± SD (n = 10/group). $^{\#\#}P < 0.01$ vs. NC, $^{**}P < 0.01$ vs. MC.

Supplemental Table 2-2. The influences of RLA8, RSV, and OCA on the body weight change and food intake in HFD -induced NASH mice.

Body weight (g)					
week	NC	MC	RSV	OCA	RLA8
1	20.45±0.50	21.03±0.52			
2	23.08±0.45	24.18±0.43			
3	24.53±0.53	25.68±0.41			
4	26.29±0.43	28.27±0.42			
5	27.05±0.42	29.65±0.50			
6	27.98±0.43	31.68±0.52			
7	28.84±0.50	33.64±0.43			
8	28.86±0.45	35.3±0.41			
9	29.76±0.53	37.24±0.45			
10	30.12±0.51	39.16±0.43			
11	30.49±0.44	41.3±0.43			
12	30.97±0.52	43.73±0.41	42.86±0.52	42.74±0.50	44.12±0.50
13	31.15±0.43	44.79±0.43$^{\#\#}$	42.34±0.44**	41.5±0.44**	42.35±0.52**
14	31.36±0.41	45.14±0.49$^{\#\#}$	43.21±0.12	41±0.41**	41.42±0.43**
15	31.69±0.42	45.4±0.53$^{\#\#}$	42.5±0.52*	41.18±0.53**	40.93±0.52**
16	32.8±0.49	45.75±0.43$^{\#\#}$	42.46±0.42*	39.97±0.43**	39.17±0.44**

Food intake (g)					
week	NC	MC	RSV	OCA	RLA8
1	3.04±0.10	2.27±0.13			
2	4.02±0.15	2.31±0.12			
3	4.02±0.13	2.42±0.12			
4	4.07±0.12	2.43±0.12			
5	4.06±0.12	2.52±0.13			
6	3.93±0.12	2.56±0.13			
7	3.71±0.13	2.57±0.12			
8	3.70±0.12	2.51±0.12			
9	3.67±0.13	2.54±0.13			
10	3.64±0.10	2.18±0.13			
11	3.67±0.15	2.21±0.12			
12	3.70±0.13	2.14±0.12	2.14±0.13	2.14±0.13	2.14±0.13
13	3.68±0.12	2.3±0.12	2.24±0.12	2.28±0.12	2.18±0.13
14	3.56±0.12	2.27±0.13	2.25±0.12	2.15±0.12	2.15±0.12
15	3.57±0.12	2.34±0.13	2.24±0.13	2.29±0.13	2.17±0.13

16	3.54±0.13	2.23±0.12	2.13±0.12	2.23±0.12	2.13±0.12

Values are the mean ± SD (n = 10/group). $^{\#\#}P < 0.01$ vs. NC, $^{*}P < 0.05$ and $^{**}P < 0.01$ vs. MC.

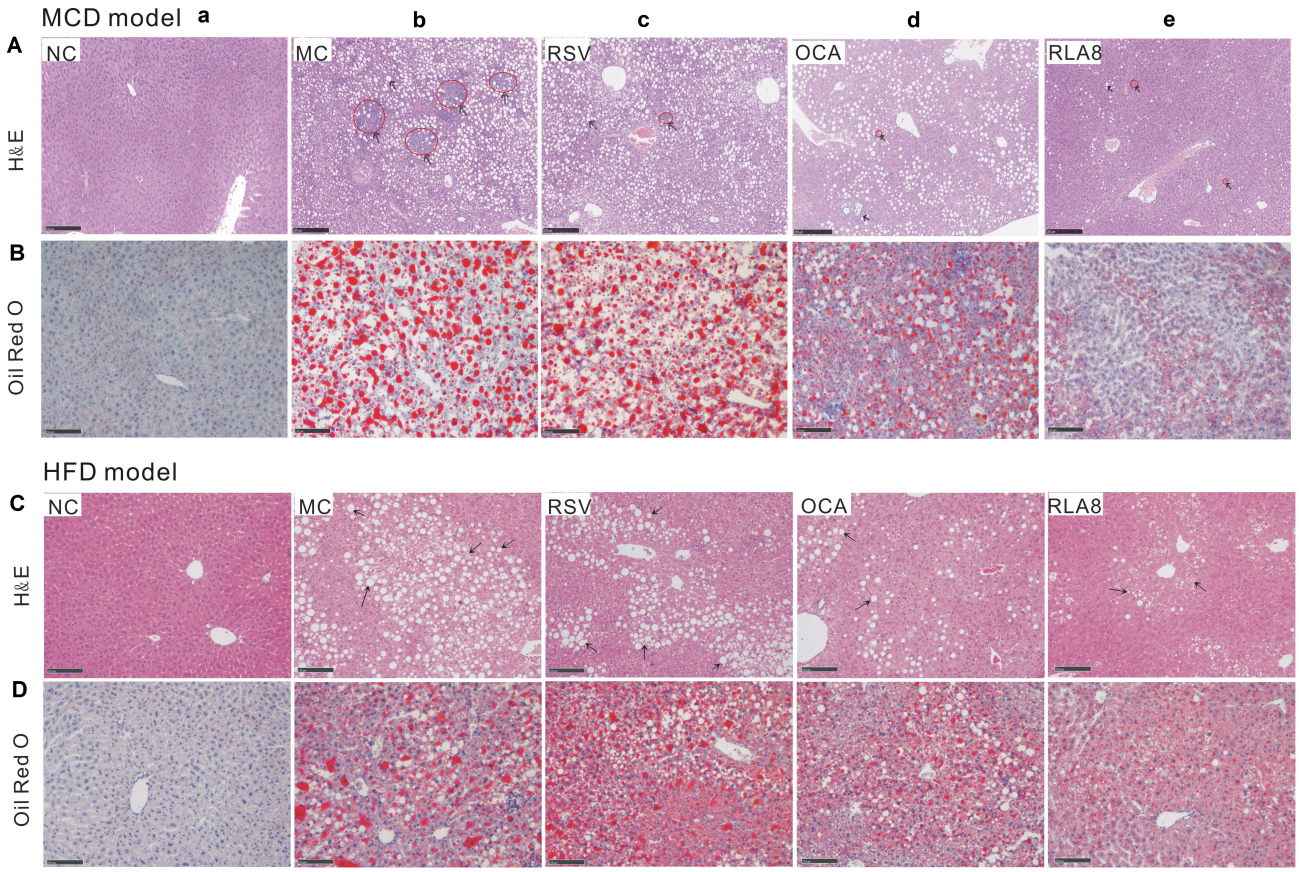

Supplemental Figure 1. The influences of RLA8, OCA, and RSV treatments on the hepatic histopathology of MCD (A) and HFD (B)-induced NASH mouse: 100×; Bar = 250 μm. Liver sections were stained with H&E and oil red O. Representative photomicrographs were obtained from the NC, MC, MCD or HFD + 100 mg/kg RSV, MCD or HFD + 10 mg/kg OCA, MCD or HFD + 100 mg/kg RLA8 groups. The black arrows indicate steatosis and the red circle with black arrows indicate necroinflammation foci.

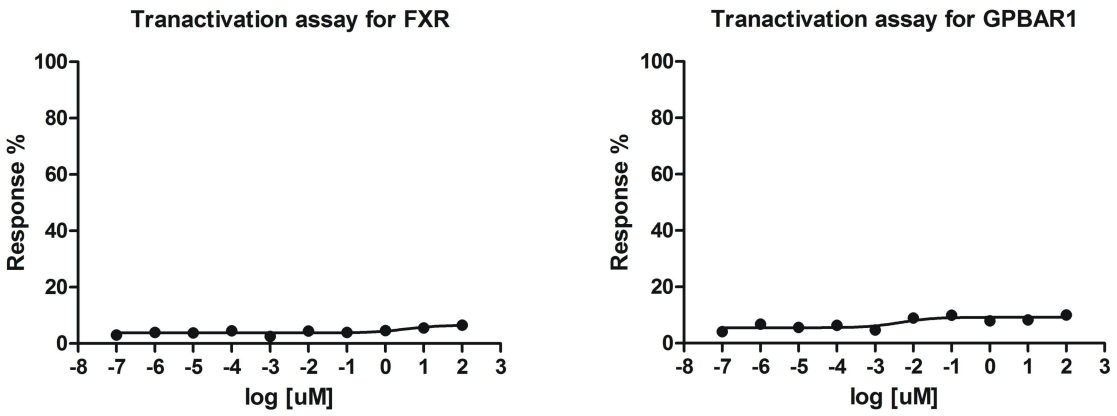

Supplemental Figure 2. The agonist activities of RLA8 for FXR and GPBAR1

Values are mean ± standard deviation (SD) that obtained from three independent experiments.